Major Urinary Proteins on Nanodiamond-Based Resonators Toward Artificial Olfaction

Emmanuel Scorsone, Raafa Manai, Maria Ricatti, Marco Redaelli, Philippe Bergonzo, Krishna Persaud, Carla Mucignat

Major Urinary Proteins on Nanodiamond Based Resonators Towards Artificial Olfaction

Emmanuel Scorsone, Raafa Manai, Maria J. Ricatti, Marco Redaelli, Philippe Bergonzo, Krishna C. Persaud, Carla Mucignat

Abstract— **A new bio-sensing platform based on Major Urinary Proteins (MUPS) from the mouse as chemical recognition elements has been developed. The transducers were surface acoustic devices coated with diamond nanoparticles as an intermediate layer enabling covalent attachment of the proteins. The resulting sensors detected 2,4-Dinitrotoluene, 4-Nitrotoluene and 2-Isobutyl-3-methoxypyrazine at ppb levels. The best sensor showed a sensitivity of 24000 Hz.ppm^{-1} to 2,4-DNT when grafted with the protein MUP20. Trends in sensitivity of the various VOC sensors were compared to the association constant values K_a of the proteins to target ligands measured by competitive assay in liquid phase. The system is able to detect analytes both in liquid as well as vapor phase and indicate that MUPs are robust bio-recognition elements that can be utilized in artificial olfaction applications.**

***Index Terms*— nanodiamond, major urinary proteins, surface acoustic wave sensors, artificial olfaction**

I. Introduction

Electronic noses based on SAW resonators have been reported for instance for the detection of coffee flavor [1], chemical warfare agents [2] or inorganic gases [3]. However, drawbacks encountered include lack of reproducibility, long-term stability and selectivity of the selective coatings deposited over the resonators [4]. The reproducibility issue arises mainly from the fact that in order to minimize damping, a very thin layer of sensing material, in the range of tens of nanometers, has to be immobilized over the resonator. Depending upon the type of sensitive coating used, which are typically polymers, it may be difficult to control the thickness at the nanoscale. An alternative approach was proposed recently that consists of depositing a thin layer of diamond nanoparticles over the transducer's surface. It was shown that rather simple chemical surface treatments of the diamond nanoparticles such as surface oxidation or hydrogenation enables tuning the sensitivity of the sensors e.g. toward polar/non polar volatile molecules [4]. Such an sp3 carbon surface may also be used as a sensing platform onto which other chemical groups with more specific affinities toward the analytes may be grafted using standard organic chemistry protocols.

E. Scorsone, R. manai and P. Bergonzo are with CEA, LIST, Diamond Sensors Laboratory, 91191, Gif-sur-Yvette, France.
M. J. Ricatti, M. Redaelli, and C. Mucignat are with the Department of Molecular Medicine, University of Padova, 35131 Padova, Italy.
K.C. persaud is with The University of Manchester, School of Chemical Engineering and Analytical Science, Oxford Road, Manchester, M13 9PL, UK

For instance the immobilization on diamond coated SAW of a Zn-porphyrin complex that is known to exhibit a high affinity to nitroaromatic compounds was demonstrated. The resulting sensor's sensitivity toward 2,4-DNT was improved by a 10-fold factor when the macromolecule was grafted onto the diamond interface instead of being casted directly over the transducer surface [5]. Moreover the sensors were found to be highly reproducible. One alternative solution investigated here is to graft over the nanodiamond bio-recognition elements that can confer a different degree of selectivity to a surface. Researchers are currently investigating the use of antibodies [6], enzymes [7], or odorant binding proteins [8] as bio receptors to be immobilized onto SAW transducers. In order to achieve a sensitive, stable, and reproducible sensor, the choice of biorecognition element is highly important. This work focuses on the investigation of Mouse Major Urinary Proteins (MUPs) as potential biorecognition elements.

MUPs are ligand binding proteins (LBP) excreted in mice urine [9]. They belong to the lipocalin family, which include many proteins able to bind a range of ligands. These proteins present a beta barrel structure with a highly hydrophobic binding pocket which retains organic molecules, allowing their transport in hydrophilic media. This family of proteins may bind small hydrophobic molecules whose features are comparable to those of explosive compounds [10]. In the mouse, MUPs are present in 21 isoforms, highly conserved in terms of biochemical characteristics and tertiary folding features and their protein sequence spans 151-187 aminoacids. However, the differences between isoforms are determined by small differences in the aminoacid sequence [11]. MUPs are involved in mouse chemical communication because they transport small odorant molecules and slowly release them in the environment [12]. For this reason, MUPs are extremely resistant to environmental challenges like heat, dehydration and proteolysis [13], making them good candidates for hybrid biosensor implementation.

The potential of lipocalin proteins as scavengers to recognize hazardous volatile compounds for the development of biosensors has been already implemented by using other lipocalin-OBPs [14, 15]. The recombinant bovine OBPs, both wild type and His-tagged mutants, were used as a scaffold to design OBP-based biosensors for detecting hazardous compounds [16]. In addition, the multifunctional properties of OBP-based devices were recently applied in an innovative filtering matrix for the removal of environmental pollutants like herbicides from water samples [17].

The present work was carried out in the framework of the European project SNIFFER aiming at developing Ligand

Binding Protein-based biosensors for border security applications, in particular for the detection of narcotics and explosives. In line with the basic concept of electronic noses and similarly to any other types of sensitive materials used for such application, it is not intended here to develop sensitive proteins that are highly specific to a single target molecule, as this is often done in medical biosensors engineering. Instead the goal is to identify a range of MUPs which will feature different affinity enough to different compounds or family of compounds to build a sensor array based system that will be able to recognize the target odors using training and pattern recognition algorithms. Here we focus on two analytes: 2,4-dinitrotoluene (2,4-DNT) and 4-nitrotoluene (4-NT), which are analogs to nitroaromatic compounds found in some explosives. Two wild type MUPs and four mutants were chemically immobilized onto diamond nanoparticle coated SAW resonators using a chemical route reported recently and involving the use of Nitriloacetic acid-Nickel complex [18]. Successful grafting was confirmed by electrochemical impedance spectroscopy on boron doped diamond electrodes. Gravimetric measurements directly on the SAW resonators enabled assessment of the surface densities of immobilized proteins. The resulting sensors were assessed in terms of sensing performances in the ppb concentration range for both 2,4-DNT and 4-NT. These were analyzed in particular comparing the affinity constants of the proteins for those analytes in liquid to the responses obtained. The experimental results are highly promising toward the use of such biosensors in electronic nose applications in general and here for homeland and border security applications.

II. MATERIALS AND METHODS

A. Preparation of major Urinary Proteins

Two wild-type MUPs (MUP3wt and MUP20wt), and 4 mutants, in which one aminoacid was changed in the MUP20wt gene sequence were used in this study (see Supplementary material 1 for details). The following mutants were analysed: MUP20L124V, MUP20Y103R, MUP20Y103D, MUP20L88Q. All mutations involve aminoacids in the binding pocket, which are critical for interactions with the ligand. The wild type 6xHis-tagged MUP20 and selected mutant genes were *in-silico* designed and purchased from Eurofins in pEAX plasmid. The plasmids carrying the gene were NdeI/EcorI (Invitrogen) digested and the agarose purified insert genes were then recombined in pET5b vector for heterologous expression in competent DE3 BL21 *E. coli* cells strain. After confirmation of the gene sequence and the induction of the bacterial expression with 0.4 mM IPTG (BioChemica, EuroClone, Milan, Italy), the protein expression was confirmed by mass spectrometry and SDS-page comparing the appropriate protein molecular weight.

TABLE 1
PROTEINS TESTED FOR BINDING TOWARDS REFERENCE COMPOUNDS EPINEPHRINE (EPIN) AND MENADIONE (MEN)

	K_d Epin	K_a Epin	K_d Men	K_a Men
MUP3	2.65±0.14	0.38 ± 0.02	0.14±0.00	6.98 ± 0.24
MUP20	5.31±0.06	0.19±0.01	0.61±0.04	1.63±0.10
MUP20L88Q	11.24±0.5	0.09 ± 0.01	1.31±0.06	0.76 ± 0.04
MUP20Y103D	3.34±0.25	0.30±0.02	0.82±0.10	1.22±0.15
MUP20Y103R	7.06±0.23	0.14 ± 0.03	1.33±0.06	0.75 ± 0.06
MUP20L124V	1.33±0.06	0.75±0.03	0.07±0.01	15.42±2.93

The proteins were purified by using the His tag system (HisTrap™ FF crude, GE Healthcare Bio-Sciences), and then concentrated and equilibrated in elution buffer (20 mM sodium phosphate, 500 mM NaCl, 500 mM imidazole, pH 7.4). The elution peak was delipidated with Sephadex LH-20 resin in acetate buffer (pH 4.5) and then dialyzed overnight against Tris 50 mM, pH 7.4. After validation of the protein structures with mass spectrometry and UV circular dichroism, *in vitro* fluorescence-competitive binding assay was performed according to a previously described protocol [19]. Protein (1μM) and the fluorescent probe N-phenyl-1-naphthylamine (1-NPN, 1.6 μM for MUP20wt and mutants; 0.6 μM for MUP3wt) were equilibrated in Tris 50 mM, pH 7.4 for 1 minute, then excited at 337 nm, the emission spectra were detected between 380-450 nm. The affinity (expressed as K_a) was measured in competitive binding assays by adding an increasing concentration of the other ligand.

All six proteins showed different K_a towards reference compounds epinephrine and menadione (see Table 1).

B. Preparation of diamond nanoparticle coated SAW resonators

The SAW transducers were supplied by the Karlsruhe Institute of Technology (KIT). They consist of 433 MHz quartz resonators with 5 μm pitch gold IDT electrodes. They were coated with diamond nanoparticles using a process described elsewhere [4], using High Pressure High Temperature (HPHT) powder Syndia™ SYP 0-0.02 supplied by Van Moppes, Switzerland. These particles feature a mean particle size of approx. 20 nm. Briefly, the layer-by-layer coating process consists of dipping the resonators in an aqueous solution of 2% wt/wt Poly(diallyldimethyl-ammonium chloride) (PDDAC) (Sigma-Aldrich, France) solution, followed by thorough rinsing in deionized water and drying under nitrogen flow. Then the resonators are dipped into a 0.1 % wt/wt colloidal solution of diamond nanoparticles. The particles of opposite charge to the polymer are thus immobilized over the surface by electrostatic interactions. The resonators are then rinsed again in deionized water and then dried. In order to increase the density of particles over the surface, the process is repeated three times overall. The diamond nanoparticles are then slightly grown by Microwave Plasma Chemical Vapor deposition (MPCVD) in a home-made reactor equipped with a 2.45 GHz-2kW Sairem microwave generator. This reactor, dedicated to synthetic diamond growth, is similar to an Astex PDS system. It is a full metal double wall reactor. The particles are grown during approximately for 30 min using the following conditions: pressure 20 mbar, gas ratio: 1% methane in hydrogen, MW power 500 W, substrate temperature 500 °C. Under those conditions the quartz resonators do not surpass the Curie

temperature and the piezoelectric properties of the material are not affected. This process allows fixing the particles over the transducer's surface and results in hydrogen surface termination of the diamond nanoparticle layer.

The MUPs were chemically grafted onto the diamond nanoparticle coating using a process described elsewhere [18]. Here the SAW resonators with hydrogen-terminated diamond surface were dipped into a 1 mM solution of Nα,Nα-Bis-(carboxymethyl)-L-lysine hydrate (≥ 97%) (NTA) for 5 min, then rinsed with deionised water and then dried under gentle N_2 flow. Here NTA forms a chemical linker between the diamond surface and the protein. Subsequently, the diamond surface was exposed to 1 mM Nickel(II) chloride hexahydrate (99.99%) solution for 2 h at room temperature resulting in NTA·Ni^{2+} complex formation. This complex has a high affinity with histidine groups. This feature has been exploited for many years for the purification of proteins. Hence the 6-His tagged MUPs were finally immobilized over the sensor surface by exposing the NTA·Ni^{2+} grafted sensors to a solutions of 1.0 mg/mL MUPs in 20 mM PBS, pH 8.00 for 2 hours. Finally the sensors were rinsed with deionised water and allowed to dry in ambient conditions.

C. Protein immobilization characterizations

Electrochemical impedance spectroscopy was used to investigate the characteristics of immobilization of the proteins. EIS requires the use of conducting diamond. Hence boron doped diamond electrodes were grown for this purpose by CVD using a process described in previous work [18]. The electrochemical characterizations were carried out in a 3 electrodes setup where BDD is the working electrode, and platinum wires both the counter and pseudo-reference electrodes, respectively. Ultrapure deionised water (Millipore Direct Q3) was used to make all the solutions. EIS was carried out in equimolar (1 mM) potassium ferricyanide(III)/ potassium hexacyanoferrate(II) trihydrate (Acros Organics) dissolved in 0.5 M potassium chloride solution (Acros Organics). The specific transfer resistances (Rt) were experimentally determined before and after each immobilization step by EIS over a frequency range of 50 kHz – 10 mHz with logarithmic point spacing and potential amplitude of 0.01 V root-mean-square (rms) while the BDD electrode was maintained at open circuit potential. EIS spectra were recorded after each grafting step. Nyquist plots were also recorded with oxidized diamond electrodes, used as negative control since in the experimental conditions used the amine terminated primary linker (NTA) can only be immobilized on hydrogen terminated surfaces [20].

Furthermore, the frequency spectra of the resonators after the immobilization steps were recorded using a network analyzer (Rohde & Schwarz ZVB20) in order to follow the variation in resonance frequency according to surface density of immobilized proteins over the surface. The mass deposited onto the transducer may be assessed according to equation 1 [8]:

$$\Delta f = (k_1 + k_2) f_0^2 \frac{m}{A} \quad \text{(eq.1)}$$

where f_0 is the fundamental resonance frequency, k_1 and k_2 are intrinsic constants of the piezoelectric substrate (here for quartz $k_1 = -8.7 \times 10^{-8}$ and $k_2 = -3.9 \times 10^{-8}$ for ST-cut quartz) [21], Δf is the frequency shift arising from mass load m, and A is the active surface area of the resonator.

D. Gas sensing measurements

Gas sensing measurements were carried out using a SAGAS instrument purchased from the Karlsruhe Institute of Technology (KIT). This instrument allows real time data acquisition simultaneously from 8 channels. All chemicals were purchased from Sigma-Aldrich, France, and used as received. 3-Isobutyl-2-methoxypyrazine (IBMP) vapors were generated using home-made permeation tubes made of ¼" external diameter PFA tubing sealed at both ends using stainless steel beads. The tubes were placed in a permeation oven from Calibrage, France. The vapor concentrations were calibrated by gravimetric analysis by measuring the weight loss of the tube every second day for two weeks. The concentrations reaching the gas cell were also double checked using a PID Photoscan instrument. The vapors coming out of the oven at constant flow of 100 sccm could be further diluted using a home-made gas rig as described elsewhere [4]. IBMP was used as reference compound as it is well known to exhibit a high affinity with most odorant binding proteins. 2,4-DNT and 4-NT vapors were generated using a similar process. This time the organic powders were placed in a crucible directly in the permeation oven. The vapor concentrations were calibrated by gravimetric analysis. The carrier gas used throughout all experiments was dry nitrogen.

III. THEORETICAL BACKGROUND

The thermodynamic dissociation constant K_d (M) may be expressed as [22, 23]:

$$K_d = \frac{[R]_0[L]_{eq}}{[LR]_{eq}} - [L]_{eq} = \frac{[R]_0[L]_0}{[LR]_{eq}} - [L]_0 \quad \text{(eq.2)}$$

Where $[L]_0$ and $[R]_0$ are the initial concentrations of free ligand and free receptor, respectively. The concentration of receptors bound at equilibrium may thus be defined by eq.3 as:

$$[LR]_{eq} = \frac{[R]_0[L]_0}{K_d + [L]_0} \quad \text{(eq.3)}$$

Assuming that the proteins are arranged in a monolayer over the sensor surface and that the adsorption model follows the Langmuir isotherm [24, 25] eq. 3 may be rewritten to express the binding saturation ratio as:

$$\upsilon = \frac{[C]}{[L]_0} = \frac{[L]_0}{K_d + [L]_0} \quad \text{(eq.4)}$$

where υ is the fractional amount of saturated proteins with a ligand within their binding pocket. This ratio can be expressed as a function of time by:

$$\upsilon(t) = \upsilon_{eq}\left(1 - e^{-t/\tau}\right) \quad \text{(eq.5)}$$

$$\upsilon_{eq} = \frac{\alpha[L]}{1+\alpha[L]} \quad \text{(eq.6)}$$

where α is the ratio $\frac{k_+}{k_-}$, and τ is the time constant defined by:

$$\frac{1}{\tau} = k_+[L] + k_- \text{ (eq.7)}$$

The thermodynamic association constant K_a (M^{-1}), also called « affinity constant » is linked to k- and k+ by equation:

$$\frac{k_-}{k_+} = K_d = \frac{1}{K_a} \quad \text{(eq.8)}$$

IV. Results and Discussion

A. Electrochemical impedance spectroscopy

The electrode transfer resistance Rt was measured before and after each grafting step both onto an as-grown BDD electrode and another diamond electrode which had been previously oxidized by ozone/UV treatment using an excimer lamp. The first electrode features a hydrogen terminated surface which has the ability to bind covalently primary amine terminated alkyl groups [20]. The latter electrode is used as negative control since the chemical binding reaction involved here is not possible on the oxidized surface. Typical impedance spectra are shown in Fig.1. Rt determination was carried out as described in reference [18].

TABLE 2
Rt values extracted from EIS for oxidized and H-terminated diamond surfaces for pristine electrodes, electrodes grafted with NTA-Ni, and electrodes grafted with NTA-Ni-6HisMUP20, respectively (mean values over 5 measurements, errors being the calculated standard deviation values)

	Oxidized BDD electrode	H-terminated BDD electrode
Pristine electrode	87 ± 12	92 ± 10
Electrode grafted with NTA-Ni	93 ± 19	293 ± 90
Electrode grafted with NTA-Ni-6HisMUP20	118 ± 25	1419 ± 20

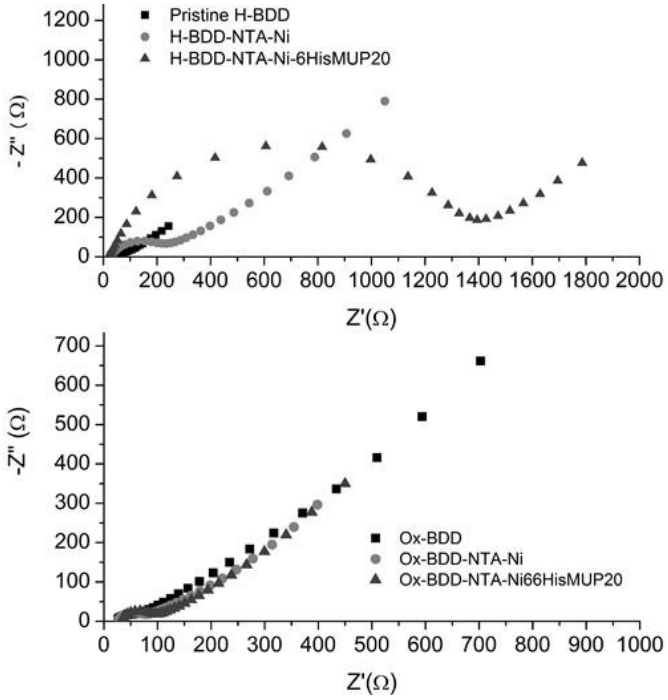

Fig.1 Typical impedance spectra of H-terminated diamond (top) and oxidized diamond (bottom) electrodes following the subsequent immobilization of NTA-Ni and then 6His-MUP20

Electron transfer for $Fe(CN)_6^{-3/-4}$ proceeds by an inner-sphere transfer mechanism where the electron transfer kinetics is highly sensitive to the electrode surface conditions. Thus the presence of immobilized organic species over the electrode surface causes a significant decrease in the electron transfer rate and therefore an increase in Rt. When no reaction occurs in the case of the oxidized electrode, the Rt value remains constant. It can be seen in Table 2 that in the case of the hydrogen-terminated electrode, Rt increases significantly from the blank hydrogen terminated surface to the NTA-Ni grafted sample, typically from 92 Ω to 293 Ω, respectively. Then a much larger increase is observed up to 1419 Ω with the same electrode upon 6hisMUP20 immobilization. In the case of the oxidized electrode, no significant variation in Rt is observed throughout the various grafting steps. Those results support that 6hisMUP20 immobilization was indeed successful on H-terminated diamond.

TABLE 3
Mean surface densities of NTA, Ni, and 6-His-MUP20 immobilized onto diamond coated SAW resonators and associated frequency shifts

Grafted chemical group	Δf (kHz)	σ (kHz)	Mean surface density (molecules/μm²)	RSD density (%)
NTA	312	± 87	$3.34x10^7$	27
Ni	131	± 49	$4.95x10^7$	38
6-His-MUP20	644	± 109	$7.53x10^5$	17

B. Gravimetric assessment of grafting density

Typical resonance spectra of a diamond coated SAW resonator before any immobilization and then following subsequent immobilization of NTA, Ni, and 6hisMUP20 are shown in Fig.2. The resonance frequency of the raw resonator

without chemical immobilization was in the order of 434.7 MHz. A shift toward the lower frequencies is clearly observed following each new immobilization step. This shift is particularly large in the case of protein immobilization (-1087 kHz from the initial resonance frequency f_0) and is followed here by a decrease in attenuation of typically -7 dB. The quality factor of the resonator was also decreased from typically 3500 to 1700 from the blank diamond coated resonator to the MUP grafted resonator, respectively. The mean surface density of NTA (MW 262.26 g.mol^{-1}), Ni and 6hisMUP20 was calculated using equation 1 and the results are summarized in Table 3. The surface density of NTA and Ni are very close to each other: 3.34x10^7 and 4.95x10^7 molecule/µm^2, respectively. This is consistent with the 1:1 stoichiometry of the ligand reported in the literature and confirmed by XPS analysis in previous work [18]. Since the amount of Ni is larger than that of NTA, it can be suggested that a small amount of non-chelated Ni is present over the surface or that the presence of NTA over the surface induces some viscoelastic contributions at the resonator surface, which are not taken into account in equation 1.

The density of 6hisMUP20 is typically two orders of magnitude below that of the linker. This is most probably due to the large size of the protein when compared to NTA. The surface densities for all immobilized MUPs are summarized in Table 4. These are generally close to 8x10^5 molecules/µm^2 for all proteins. This value is approximately 10 times higher than when Odorant Binding Proteins of similar sizes are immobilized onto the gold surface of SAW devices [8].

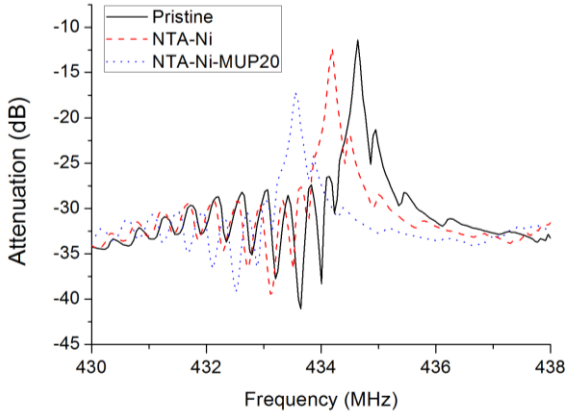

Fig.2 Typical frequency spectra of diamond coated resonators with a: no chemical grafting, b: NTA, c: NTA-Ni, and c: NTA-Ni-6hisMUP20

C. *Gas sensing performances*

The typical responses of three sensor replicates grafted with 6hisMUP20L88Q to five successive exposures to 18 ppm IBMP vapor in dry nitrogen are shown in Fig.3. The curves show that the response is fairly fast and fully reversible. The T90% response time for such sensor here was found to be in the order of 200 seconds. Moreover, the response signal intensity is both repeatable and reproducible. No significant drift in the response was observed after 5 cycles. The signal intensity variations at the steady state response from sensor to sensor for a given exposure were found to be typically below 12%. Sensors grafted with 6hisMUPL88Q were exposed successively to increasing concentrations of IBMP, 2,4-DNT and 4-NT and the time constants τ from the inverse exponential responses were extracted. 1/τ was plotted as a

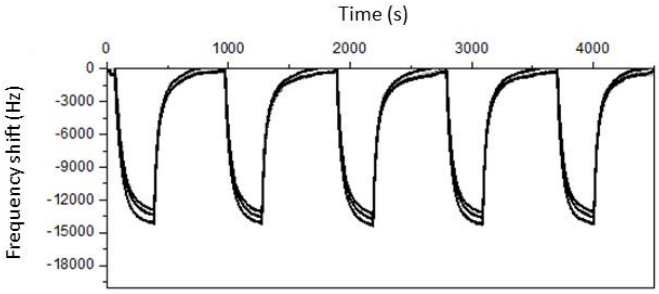

Fig.3. Typical transient response of three separate 6hisMUP20L88Q grafted diamond SAW sensors to cyclic exposures to 18 ppm IBMP in dry nitrogen

function of the concentration of ligand and for each vapor a linear model was fitted to the data points. These plots are shown in Fig.4 a, b, c. According to eq. 7, the slopes of the lines correspond to k+ and the y-intercept to k- values, respectively. Subsequently, the values of the thermodynamic association constants can be derived from eq. 8. These values are summarized in Table 5 and compared with the K_a values obtained by competitive binding assay achieved in liquid from the same batch of proteins. The higher the K_a values, the higher the sensitivity is expected since more ligands are chelated with the receptor. Hence, according to Table 5, the sensor grafted with MUP20 seems to have in the gas phase a sensitivity increasing in the order IBMP<2,4-DNT<4-NT. Interestingly, the Ka values for the nitroaromatic compounds is much higher than for IBMP, which is generally known to exhibit a good affinity with most LBPs. This trend is different in the liquid phase, where the affinity to IBMP is slightly higher than for the nitroaromatics. Nevertheless in liquid differences in K_a values are much lower than in the gas phase and closer to each other (see Supplementary S2).

TABLE 4
GRAFTING DENSITIES OF MUP IMMOBILIZED ONTO DIAMOND COATED SAW RESONATORS

Protein	Weight KDa	Grafting density (kg/m^2)	Grafting density Molecules/µm^2
6his-MUP3	21	2.79x10^{-5}	8.00x10^5
6his-MUP20	21.9	2.73x10^{-5}	7.53x10^5
6his-MUP20-Y103R	20.5	2.86x10^{-5}	8.40x10^5
6his-MUP20-Y103D	20.5	2.85x10^{-5}	8.37x10^5
6his-MUP20-L88Q	20.5	2.73x10^{-5}	8.02x10^5
6his-MUP20-L124V	20.5	2.84x10^{-5}	8.34x10^5

TABLE 5
AFFINITY CONSTANTS EXTRACTED FROM EXPERIMENTAL DATA FOR 6HISMUP20

	k+ (mol^{-1} s^{-1})	k- (s^{-1})	Ka (mol^{-1})	Ka (mol) – liquid
IBMP	2.95x10^{-3}	8.66x10^{-3}	0.34	0.77
2,4-DNT	3.49x10^{-2}	4.57x10^{-3}	7.64	0.26
4-NT	6.89x10^{-3}	7.85x10^{-4}	8.78	0.45

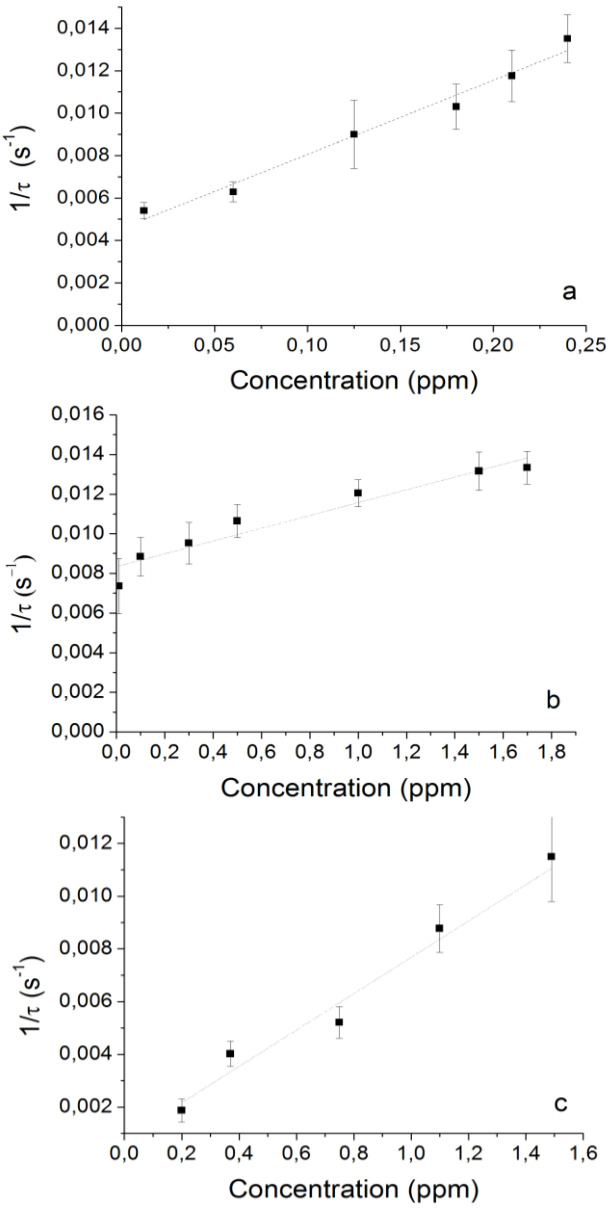

Fig.4. Plots of 1/τ versus concentration, with τ being the time constant of reverse exponential responses after reaching steady state for each concentration, for a: IBMP exposures, b: 2,4-DNT exposures, and c: 4-NT exposures

One has to keep in mind here that the latter values are obtained by competitive binding. In this case, although the affinity constants may be compared for various ligands because they are recorded in the same experimental conditions, one has to be careful when comparing these K_a values with those recorded in the gas phase, since in liquid the ligand is in competition with the fluorescent probe and therefore the results depend also upon the affinity of the receptor with the probe.

Next, the whole series of MUP were exposed to increasing concentrations of IBMP, 2,4-DNT, and 4-NT in the range 0-2 ppm, 0-250 ppb and 0-1.5 ppm respectively. Examples of transient responses and resulting calibration curves are shown in supplementary material 3 for selected proteins. All sensors exhibit a fairly linear response in the investigated concentration ranges. The highest sensitivities are obtained toward 2,4-DNT vapors. The most sensitive sensor, grafted with MUP20L124V, exhibits sensitivity as high as 24606 Hz/ppm. Quite interestingly, the sensitivity of the various MUPs toward IBMP is significantly lower than for nitro aromatics, as observed previously from the data in Table 5. The sensitivity values were plotted along with K_a values recorded by competitive binding in liquid in Fig. 5 a, b, and c in an attempt to compare the trends for both parameters and to see whether some correlation does exist between the affinity constants of the proteins in aqueous environment and their vapor sensitivity in air.

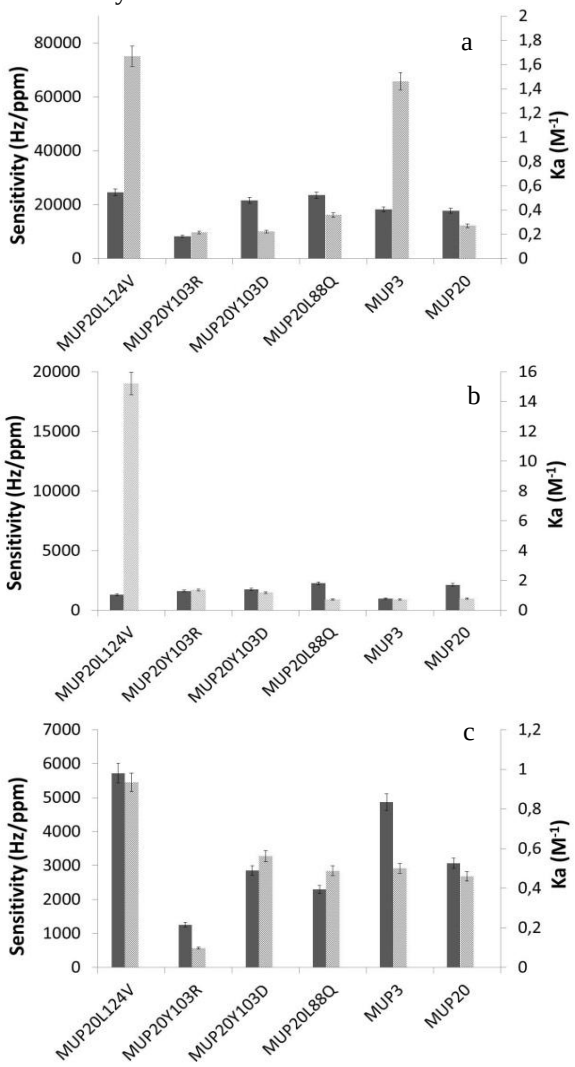

Fig.5. comparison between Ka values recorded by competitive binding in liquid (light grey) and sensitivity values recorded in the gas phase for a: IBMP, b: 2,4-DNT and c: 4-NT (dark grey).

Both trends generally follow each other fairly well, with three major exceptions: the affinity constants K_a for MUP20L124V and MUP3 for 2,4-DNT and the affinity constant for MUP20L124V for IBMP, respectively, are significantly much higher than for the other MUP but do not result in higher relative sensitivities. Several hypotheses may explain this observation: (i) when immobilized on the sensor surface, the protein may undertake conformal changes, in particular because it evolves in a dry environment, which may affect its

ability to bind the ligand, (ii) conformal changes of some proteins on binding the ligand may be impeded because of steric effects or other neighboring protein to protein interactions, especially for dense layers of immobilized protein, which may also affect the sensitivity of some sensors. Apart from this, the evidence indicates that there is a good correlation between the K_a values in liquid and the sensitivities in the gas phase.

V. Conclusion

Major Urinary Proteins were immobilized for the first time over the surface of acoustic wave resonators and used as sensitive coatings for the detection of small volatile organic compounds, namely 2,4-DNT and 4-NT, which are analogs to nitroaromatic compounds entering in the composition of artisanal explosives. IBMP was also used for comparison. The proteins were immobilized successfully over the surface of the transducers using a diamond nanoparticle interlayer enabling attachment of the receptors via covalent bonding of NTA followed by chelating with Nickel via the 6His tag of the proteins. The density of immobilized MUP20 was assessed by gravimetric measurements using SAW transducers and was found to be typically an order of magnitude higher than when other similar LBPs were immobilized on gold surfaces. Six different MUPs were used and assessed in terms of sensing performances against the analytes. Higher sensitivities were generally observed for the nitroaromatic compounds, and in particular 2,4-DNT. Here the sensitivity ranged from typically 8000 Hz/ppm to 24000 Hz/ppm depending on the MUP tested. The sensitivities of the various sensors were compared to the association constant of the various MUPs recorded by competitive assay in liquid. For most proteins, the same trend in intensity seemed to be observed between the sensitivity and Ka values. These results demonstrate the high potential of MUPs for the detection of explosive vapors for security applications and more generally for the detection of small volatile organics in the area of artificial olfaction.

Acknowledgment

Financial support from the European Commission Research Innovation - 7th Framework Program (FP7-SECURITY project n° 285203) is gratefully acknowledged.

References

[1] N. Barié, M. Bücking, U. Stahl, M. Rapp, "Detection of coffee flavour ageing by solid-phase microextraction/surface acoustic wave sensor array technique (SPME/SAW)", *Food Chemistry*, vol. 176, pp. 212-218, 2015.

[2] F. Di Pietrantonio, M. Benetti, D. Cannatà, E. Verona, A. Palla-Papavlu, V. Dinca, M. Dinescu, T. Mattle, T. Lippert, "Volatile toxic compound detection by surface acoustic wave sensor array coated with chemoselective polymers deposited by laser induced forward transfer: Application to sarin", *Sensors and Actuators B*, vol.174, pp. 158-167, 2012.

[3] M. Asada, M. H. Sheikhi, "Surface acoustic wave based H_2S gas sensors incorporating sensitive layers of single wall carbon nanotubes decorated with Cu nanoparticles", *Sensors and Actuators B*, vol. 198, pp. 134-141, 2014.

[4] E. Chevallier, E. Scorsone, P. Bergonzo, "New sensitive coating based on modified diamond nanoparticles for chemical SAW sensors", *Sensors and Actuators B*, vol. 154, pp. 238-244, 2011.

[5] E. Chevallier, E. Scorsone, H.A. Girard, V. Pichot, D. Spitzer, P. Bergonzo, "Metalloporphyrin-functionalised diamond nano-particles as sensitive layer for nitroaromatic vapors detection at room-temperature", *Sensors and Actuators B*, vol. 151, pp. 191-197, 2010.

[6] S. Rupp, M. von Schickfus, S. Hunklinger, H. Eipel, A. Priebe, D. Enders, A. Pucci, "A shear horizontal surface acoustic wave sensor for the detection of antigen–antibody reactions for medical diagnosis", *Sensors and Actuators B*, vol. 134, pp. 225–229, 2008.

[7] D. Liu, L. Nie, S. Yao, "Kinetic analysis of arginase-urease coupled reaction with a surface acoustic wave enzyme sensor system", *Talanta*, vol. 43, pp. 667-674, 1996.

[8] F. Di Pietrantonio, D. Cannata, M. Benetti, E. Verona, A. Varriale, M. Staiano, S. D'Auria, "Detection of odorant molecules via surface acoustic wave biosensor array based on odorant-binding proteins", *Biosensors and Bioelectronics*, vol. 41, pp. 328-334, 2013.

[9] Z. Böcskei, C.R. Groom, D.R. Flower, C.E. Wright, S.E Phillips, A. Cavaggioni, J.B. Findlay, A.C North, "Pheromone binding to two rodent urinary proteins revealed by X-ray crystallography". *Nature*, 360(6400), pp. 186-8, 1992.

[10] D.R. Flower, "The lipocalin protein family: structure and function". *Biochem J.*, vol. 318 (Pt 1), pp. 1–14, 1996.

[11] S.D. Sharrow, J.L. Vaughn, L. Zídek, M.V. Novotny, M.J. Stone, "Pheromone binding by polymorphic mouse major urinary proteins". *Protein Sci.*, vol. 11(9), pp. 2247-56, 2002.

[12] A. Cavaggioni, C. Mucignat, R. Tirindelli, "Pheromone signalling in the mouse: role of urinary proteins and vomeronasal organ". *Arch Ital Biol*., vol. 137(2-3), pp. 193-200, 1999.

[13] C. Mucignat-Caretta; A. Caretta, "Message in a bottle: major urinary proteins and their multiple roles in mouse intraspecific chemical communication", *Animal Behaviour*, vol. 97, pp. 255-263, 2014.

[14] H.H. Meng, B.Caddy, "Gunshot residue analysis-a review". J Forensic Sci., pp. 542-553, 1997.

[15] M. Tegoni, P. Pelosi, F. Vincent, S. Spinelli, V. Campanacci, S. Grolli, R. Ramoni, C. Cambillau, "Mammalian odorant binding proteins" *Biochim. Biophys Acta*., vol. 1482, pp. 229–40, 2000.

[16] R. Ramoni, S. Bellucci, I. Grycznyski, Z. Grycznyski, S. Grolli, M. Staiano, G. De Bellis, F. Micciulla, R. Pastore, A. Tiberia, V. Conti, E. Merli, A. Varriale, M. Rossi, S. D'Auria, "The protein scaffold of the lipocalin odorant-binding protein is suitable for the design of new biosensors for the detection of explosive components*", J. Phys. Condens. Matter*., vol. 19, pp. 395012-395013, 2007.

[17] F. Bianchi, G. Basini, S. Grolli, V. Conti, F. Bianchi, F. Grasselli, M. Careri, R. Ramoni, "An innovative bovine odorant binding protein-based filtering cartridge for the removal of triazine herbicides from water". *Anal Bioanal Chem.* , vol. 405(2-3), pp. 1067-1075, 2013.

[18] R. Manai, E. Scorsone, L. Rousseau, F. Ghassemi, M. Possas Abreu, G. Lissorgues, N. Tremillon, H. Ginisty, J-C. Arnault, E. Tuccori, M. Bernabei, K. Cali, K.C. Persaud, P. Bergonzo, "Grafting odorant binding proteins on diamond bio-MEMS", *Biosensors and Bioelectronics*, vol. 60, pp. 311-317, 2014.

[19] Y.F. Sun, F. De Biasio, H.L. Qiao, I. Iovinella, S.X.Yang, Y Ling, L. Riviello, D. Battaglia, P. Falabella, X.L. Yang, P. Pelosi, "Two odorant-binding proteins mediate the behavioural response of aphids to the alarm pheromone (E)-ß-farnesene and structural analogues". *PLoS One*.. 7(3):e32759, 2012.

[20] C. Agnès, S. Ruffinatto, E. Delbarre, A. Roget, J-C. Arnault, F. Omnès, P. Mailley, "New one step functionalization of polycrystalline diamond films using amine derivatives", *IOP Conf. Series: Mater. Sci. Eng.*, vol. 16, pp. 012001, 2010.

[21] J.W. Grate, M. Klusty, Analytical Chemistry, 63 (17), 1719–1727, 1991.

[22]. A. F. Williams, "Cellular Interactions - out of Equilibrium". *Nature*, vol. 352, pp. 473-474, 1991.

[23] J. Kubi, Immunology. W. H. Freeman and Company: New York, 1994.

[24] Langmuir I. The adsorption of gases on plane surfaces of glass, mica and platinum, *J. Am. Chem. Soc*., vol. 40, pp. 1361-1403, 1918.

[25] A. W. Adamson, Physical chemistry of surfaces, 5th edition, Wiley: New York, 1990.